Int. J. Electrochem. Sci., 12 **(2017)** 374 – 385, doi: 10.20964/2017.01.53

International Journal of
ELECTROCHEMICAL
SCIENCE
www.electrochemsci.org

Short Communication

Preparation of Yttrium-based Rare Earth Conversion Coating and Its Effect on Corrosion Resistance of AZ91D Magnesium Alloy

Baojun Han[1,2,], Dongdong Gu[2], Yang Yang[2], Ling Fang[1,2], Guanghuai Peng[1,2], Chubin Yang[1,2]*

[1] Jiangxi Provincial Engineering Research Center for Magnesium alloys, GanNan Normal University, Ganzhou 341000, PR China
[2] School of Chemistry and Chemical Engineering, GanNan Normal University, Ganzhou 341000, PR China
[*]E-mail: bao77junhan@yahoo.com

Received: 10 October 2016 / *Accepted:* 16 November 2016 / *Published:* 12 December 2016

The yttrium-based rare earth conversion coating on the surface of AZ91D magnesium alloy was prepared and post-treated by simple immersing in solution of yttrium nitrate ($Y(NO_3)_3$) and silica sol. The micro-morphology, transverse section and composition of the coatings were investigated by scanning electron microscopy (SEM), energy dispersive spectroscopy (EDS) and X-ray photoelectron spectroscopy (XPS), respectively. The corrosion resistance was assessed by means of potentiodynamic polarization curves, immersion testing and electrochemical impedance spectroscopy (EIS). The results show that the coating is mainly composed of Y_2O_3, YOx/y, Al_2O_3 and MgO, and the post-treated yttrium-based rare earth conversion coating was homogeneous and uniform in morphology. The corrosion resistance capability of the coated AZ91D magnesium alloy was obviously improved compared with the bare one. The corrosion potential shifted positively about 230 mV, and the corrosion current density decreased about two orders of magnitude.

Keywords: yttrium-based conversion coating; AZ91D magnesium alloy; rare earth; post-treatment; corrosion resistance

1. INTRODUCTION

Mg is the lightest structural metallic material with many excellent properties, such as low density, good casting ability, favorable bio-compatibility etc. [1], and there is a growing interest in applying it in many fields including electronics, automobile and aerospace industries. One of the biggest disadvantages of magnesium and its alloys is their poor corrosion resistance in even mild environments, which seriously limits their applications in diverse fields [2,3]. Surface modification

treatment is one of the most promising methods to solve the corrosion problem of Mg and its alloys. The protection layer can be conversion coatings or coatings prepared through anodizing, vapor phase deposition, spinning organic coatings and electro-less plating etc. [4-13]. Among these methods, coatings prepared by chemical conversion treatment have attracted much attention for its low cost, uniform deposition structure, and simplicity in operation. The conventionally used conversion coatings are usually based on chromium compounds that have been proven to be highly toxic carcinogens. Therefore, it is imperative to develop new environment-friendly conversion treatments for Mg alloys. The rare earth based conversion coatings [14-16] are considered to be one of the best candidate for replacing the hexavalent chromium compounds for its low toxicity [17,18]. In previous works, the addition of rare earth La and Ce were widely adopted to improve the corrosion resistance capability of Mg alloys, Al alloys and Zn alloys [19-21]. But there are few reports about the application of other rare earth elements such as Y, Gd and Nd in preparation of chemical conversion coatings. Besides, there are large amount of micro-cracks in the rare earth element-based conversion coatings, and which seriously decrease the corrosion resistance capability of the coatings [22,23]. Chol etc. [24] improved the corrosion resistance of the AZ31 magnesium alloy by simple stannite post-treatment, and Sol-gel technique [25-28] was also used to seal the micro-cracks of the conversion coating, which have a positive effect on the interlayer.

In present work, the yttrium-based rare earth conversion coating on AZ91D Mg alloys was fabricated firstly, and then post-treated by simple SiO_2 sol sealing technique to heal the micro-cracks on the coating. The microstructure, chemical composition and the corrosion-resistance capability of the as-prepared conversion coatings and after crack-remediation were investigated, and the formation mechanism of the anticorrosion coatings on the Mg alloys was discussed.

2. EXPERIMENTAL

2.1 Materials and coating preparation

The substrate material used in present study was AZ91D magnesium alloy with a chemical composition of Mg-9.2Al-0.5Zn (wt. %). The samples were first polished using water-proof abrasive paper from 180 down to 2500 grits, and then a diamond paste of 3.5 μm. After polishing, the samples were degreased in absolute ethanol in an ultrasonic bath for 15 min， and the samples were dipped into a HNO_3 (0.8%) aqueous solution for 15 s and subsequently dipped into a 40% HF aqueous solution for 30 s to increase the adhesion of the coating and substrate. Between each step, the samples were rinsed with distilled water in ultrasonic bath for 5 min to remove all the residues on the surface of the samples, and then dried in a stream of cold air.

The yttrium-based rare earth conversion coatings on the samples were prepared by immersing in 10 g/L yttrium nitrate $Y(NO_3)_3$ solution at 30 ℃ for different time, and the reaction vessel was placed in a magnetic stirring apparatus during coating preparation. Then the samples were thoroughly rinsed with deionized water and dried in cold air. At last, the samples, which were coated with yttrium-based rare earth conversion coatings, were dipped in a 30% mass fraction of silica sol solution and naturally dried in air for 24 h followed by heating at 250 ℃for 2 h to seal the cracks on the coatings.

2.2 Characterization

The micro-morphology and the chemical composition of the coatings were examined using a scanning electron microscopy (SEM, Quanta, FEI-450) equipped with Oxford X-ray energy dispersive spectrum (EDS). The chemical composition of the coating was probed using an X-ray photoelectron spectroscopy (XPS, Physical Electronics, Thermo ESCALAB 250Xi) with Al Kα (hν=1486.6 eV) monochromatic source, and all spectra were corrected using the signal of C 1s at 284.8 eV. The electrochemical test was conducted using a Metrohm Autolab electrochemical workstation in a three-electrode cell composed of a reference electrode (a saturated calomel electrode), a counter electrode (a platinum foil) and a working electrode. The area of the working electrode was 1.0 cm^2. EIS measurements were carried out at a certain corrosion potential in a frequency range from 10^{-2} Hz to 10^5 Hz using a 10 mV amplitude perturbation. The potentiodynamic polarization curves were performed at a scanning rate of 1 mV/s. The corrosion environment was simulated by 3.5% NaCl solution at room temperature. The immersion test was conducted in an aquarium filled with 3.5% NaCl solution for 72h at room temperature, and consequently, the samples were washed by 10% Cr_2O_3 solution for about 10 min and rinsed with demineralized water and dried in cold air.

3. RESULTS AND DISCUSSION

3.1. Formation process of yttrium-based conversion coating

Fig.1 shows the SEM surface morphology of the coatings immersed in 10g/L $Y(NO_3)_3$ at 30 ℃ for different time. It can be seen that the precipitates first deposited at the sites of eroding pits, as shown in Fig.1a. When the immersing time was increased to 10s, the size of the white products increased accordingly (Fig.1b), and the eroding pits were gradually covered by the precipitate when immersed in the solution for 30 s (Fig.1c). When the immersing time was increased to 5 min, some spherical particles were formed and some surface areas were completely covered by the coating (Fig.1d). When the immersion time was further prolonged to 20 min, a uniform conversion coating covered the whole surface of the sample (Fig.1e) but the coating was very thin. As shown in Fig.1f, the coating became uniform and thicker with immersing time increased, and some wide cracks were also formed on the coating.

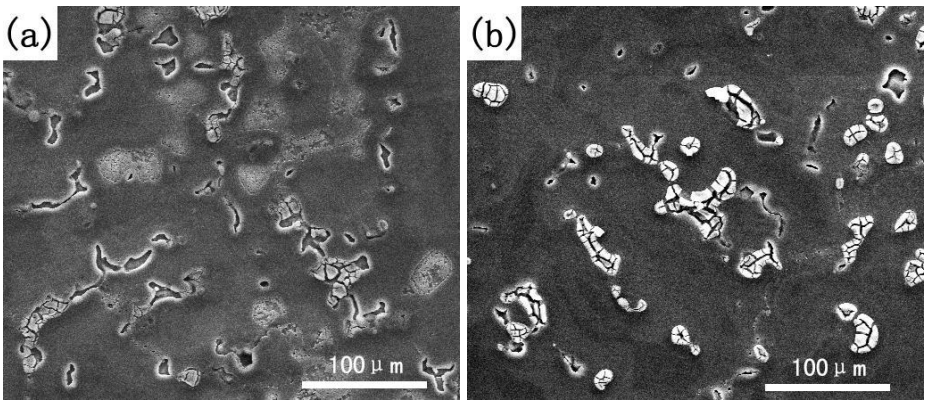

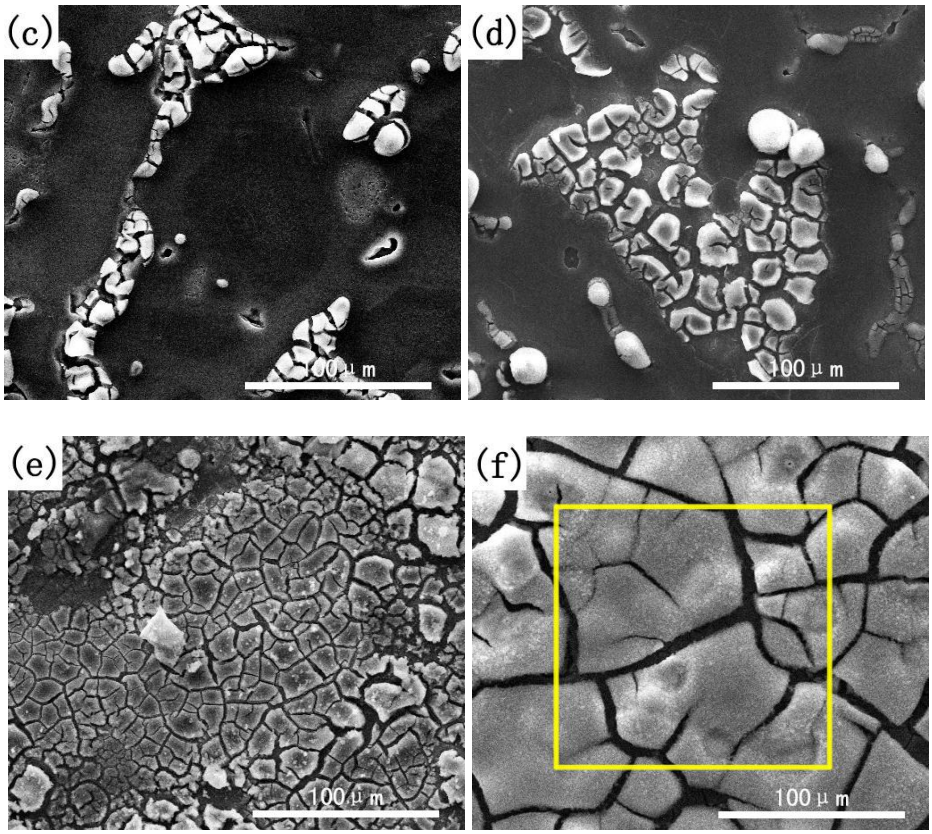

Figure 1. SEM Morphology of the yttrium-based rare earth conversion coatings on AZ91D magnesium alloy immersed in 10 g/L $Y(NO_3)_3$ solution at 30 ℃ for time of (a) 5s, (b) 10s, (c) 30s, (d) 5min, (e) 20min and (f) 50min

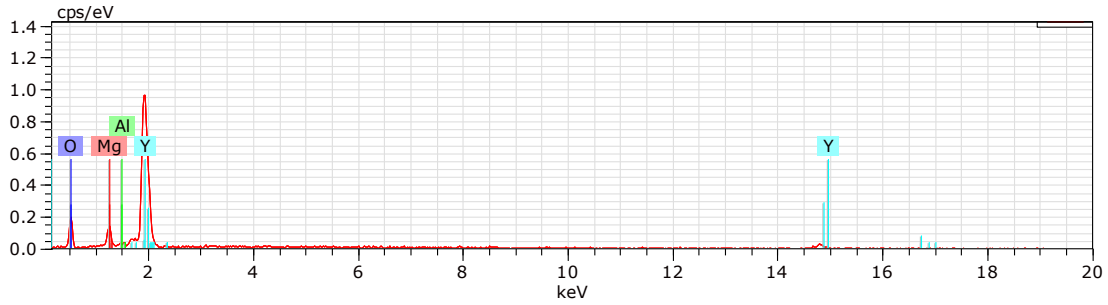

Figure 2. EDS micro area scanning result of yttrium-based conversion coating on AZ91D magnesium alloy immersed in 10 g/L $Y(NO_3)_3$ solution at 30 ℃ for 50 min (indicated by yellow box in Fig.1f)

The whole coating growing process was similar to the neodymium-based coating [29], cerium conversion coating [30]. It is considered that the cracks formed on the conversion coating is induced by hydrogen evolution and high inner stress as reported in reference [15] and [31]. Fig.2 shows the EDS spectra of the coating by micro area scanning along the yellow box in Fig.1f. The EDS results show that the coating was mainly composed element of Y, O, Al and Mg. XPS analysis was performed to evaluate the composition of the surface of the coating. As shown in Fig.3, XPS survey spectra detected Y, O, Mg, and Al peaks, which is in accordance with the EDS results. As shown in Fig.3a, the Y 3d peak can be decomposed into three peaks, which can be assigned to Y 3d3/2 and Y 3d5/2. The Y

3d3/2 and Y 3d5/2 peaks were measured at 158eV and 158.95eV, which can be attributed to Y^{3+} [32], which indicates that the conversion coating consists of YOx/y and Y_2O_3. The O 1s peak was detected at 531.3eV in Fig.3b, which is assigned to oxides. The Al 2p peak showed in Fig.3c reflects the formation of Al_2O_3. The high resolution spectrum of Mg 1s is corresponding to MgO. All these results reveal that the yttrium conversion coating is mainly composed of Y_2O_3, YOx/y, Al_2O_3 and MgO. The XPS results are consistent with the results of SEM and EDS.

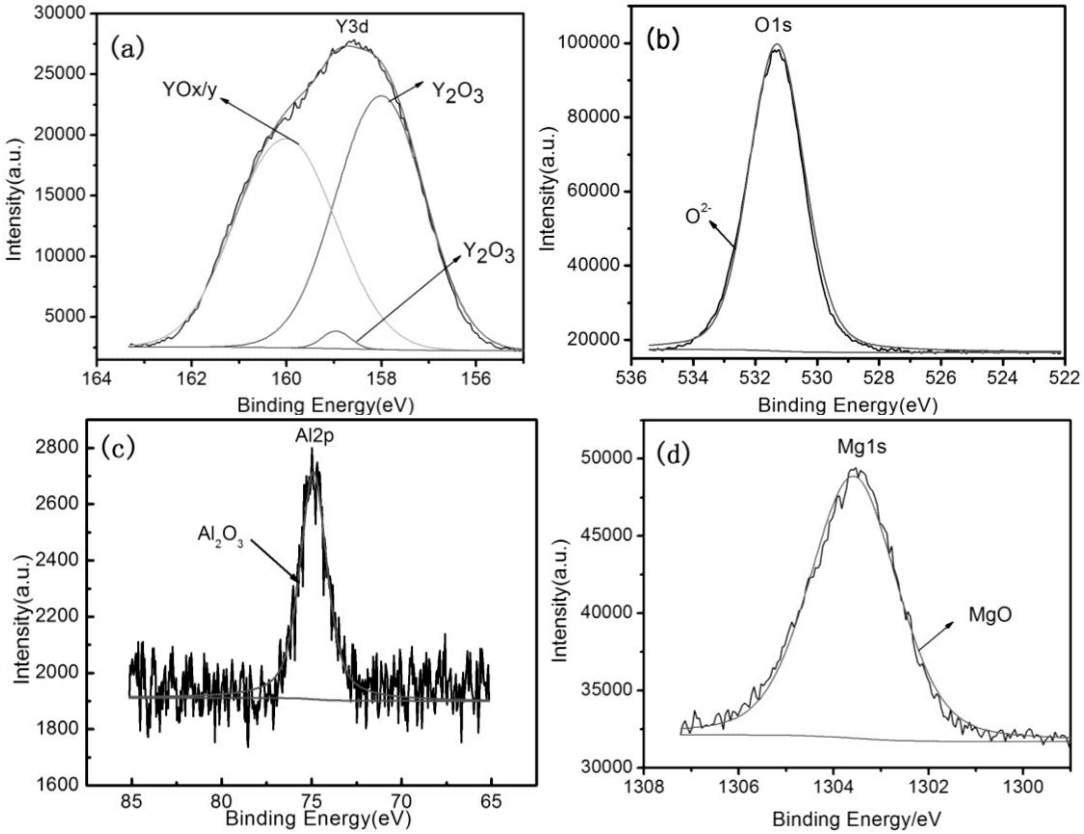

Figure 3. Decomposed XPS spectra of yttrium-based conversion coating on AZ91D magnesium alloy immersed in 10 g/L $Y(NO_3)_3$ solution at 30 ℃ for 50 min

The formation mechanism of the coating layer is related to the electrochemical reaction on metal surface. The standard electrochemical potential of β-$Al_{17}Mg_{12}$ phase is much higher than that of the α-Mg phase[332,34], which makes the Mg-rich phase in the substrate act as an active anode, and the Al-rich β phase act as an active cathode in the treating solution. The anodic reaction is the dissolution of the Mg, and the cathode reaction is the reduction of H^+ according to the following equations:

Anode reaction: $Mg \rightarrow Mg^{2+} + 2e$ (1)

Cathode reaction: $H_2O + 2e \rightarrow 2OH^- + H_2\uparrow$ (2)

Therefore, Y^{3+}, Mg^{2+} and Al^{3+} which were known as the main active ions, exists in the liquid layer of the alloy surface. The above-mentioned reactions result in an increased OH^- concentration.

The increased pH value of the local cathode sites between the substrate and the solution leads to the formation of the metal hydroxides. When the pH value in the solution rises to a certain value, hydrates coating will deposit on the sample surface. During the competitive reactions between OH^- and Al^{3+}, Y^{3+} ions, and Mg^{2+} ions, the Al^{3+} and Y^{3+} ions are more favorable to form hydroxides and deposit on the surface, because of the solubility of aluminum hydroxide, magnesium hydroxide and yttrium hydroxide is 1.3×10^{-33}, 5.61×10^{-12} and 1.0×10^{-22}, respectively. The forming reactions of the coating layer are as follows:

$$Y^{3+} + 3OH^- \rightarrow Y(OH)_3 \downarrow \quad (3)$$

$$Mg^{2+} + 2OH^- \rightarrow Mg(OH)_2 \downarrow \quad (4)$$

$$Al^{3+} + 3OH^- \rightarrow Al(OH)_3 \downarrow \quad (5)$$

The decomposition will occur when the composite conversion coating is exposed to air [35]. Therefore, it can be concluded that the yttrium conversion coating on the AZ91D alloy consists of yttrium oxide, aluminum oxide and magnesium oxide, as confirmed by the above experimental results.

3.2 Post-treatment of yttrium-based conversion coating

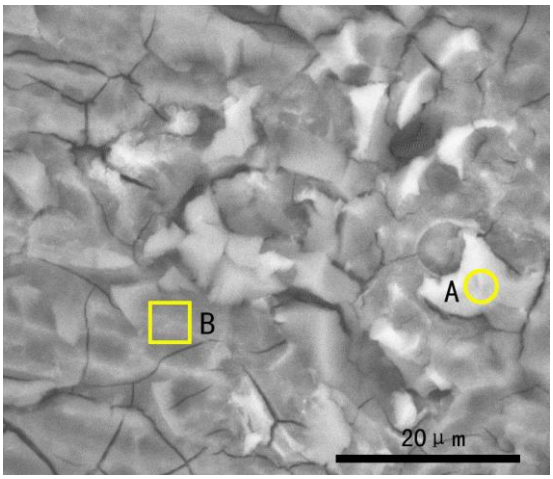

Figure 4. SEM surface morphology of the coating on AZ91D magnesium alloy immersed in 10 g/L $Y(NO_3)_3$ solution at 30 ℃ for 50 min, then dipped in 30% mass fraction of silica sol solution and naturally dried in air for 24 h followed by heating at 250 ℃ for 2 h

The post-treatment was carried out by immersing the Mg alloy with the conversion coatings into a silica sol solution to heal the cracks formed within the coatings, which may further improve the anti-corrosion property of the yttrium conversion coating by preventing the etchant penetrate through the conversion coating layer [36]. The morphology of the conversion coating after the silica sol treatment is shown in Fig.4. Table 1 lists the quantitative analysis of the chemical composition of the conversion coatings after silica sol treatment determined by EDS marked in the area of Fig.4. It can be

found that the coating is composed of elements of Mg, Si, Y, O and Al, Which means that the silica sol solution can seal the cracks and pores very well.

Table 1. EDS atomic ratios (at.%) of corresponding marked positions on the surface coating of AZ91D magnesium alloy immersed in 10 g/L $Y(NO_3)_3$ solution at 30 ℃ for 50 min, then dipped in 30% mass fraction of silica sol solution and naturally dried in air for 24 h followed by heating at 250 ℃for 2 h

Location	Mg (at.%)	Si (at.%)	O (at.%)	Y (at.%)	Al (at.%)
A	35.22	7.76	51.78	2.87	2.37
B	32.89	49.45	14.65	0.21	2.80

Fig.5 shows the morphology of the transverse section of the yttrium-based conversion coating and the sample treated in the silica sol solution. Fig.5a demonstrates that numerous cracks exist on the surface of the as-prepared conversion coating, which can behave as corrosion source when the alloy is exposed to etchant. After immersing the conversion coating into the silica sol solution, the cracks are filled with SiO_2 and no cracks through the coating can be observed. The white area is yttrium conversion coating and the gray one is SiO_2. The structure of the coatings protect the magnesium alloys from the corrosion medium in ambient. In general, the interlayer nearby the substrate would avoid the corrosion of magnesium alloys. The outer layer can seal the micro-pores and micro-cracks formed within the chemical conversion coatings. Thus, the silica sol treatment of the conversion coatings will dramatically improve the corrosion-resistance capability of the magnesium alloys.

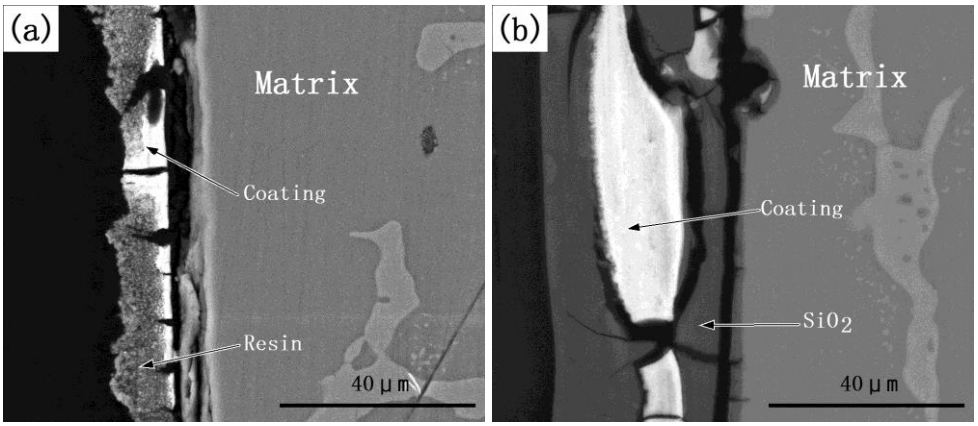

Figure 5. SEM Transverse sectional morphology of (a) the yttrium-based conversion coating immersed in 10 g/L $Y(NO_3)_3$ solution at 30 ℃ for 50 min and (b) the yttrium-based conversion coating dipped in 30% mass fraction of silica sol solution and naturally dried in air for 24 h followed by heating at 250 ℃for 2 h

3.3 Corrosion resistance of the post-treated conversion coating

The cathode reaction in the polarization curves corresponds to the evolution of the hydrogen. The anodic polarization curve shows important features related to the corrosion resistance [37]. Fig.6 shows the polarization curves of the blank sample, the yttrium-based conversing coating and the yttrium-based conversing coating after treatment by the silica sol solution in 3.5 wt.% NaCl solution at room temperature. It can be found that the hydrogen evolution rate decreased seriously after the treatment of the conversion coating on the AZ91D magnesium alloy with the silica sol. The corrosion current density of the bare alloy increased sharply with the increasing potentials, indicating the corrosion of the magnesium substrate [38] and the conversion coating. In a typical polarization curve, low corrosion current densities correspond to good capability of resisting corrosion. It can be found from the polarization curves in Fig.6 that the silica sol-treated coating slows down the corrosion rate of the conversion coating by inhibiting both the cathodic hydrogen evolution and the anodic dissolution reactions. The E_{corr} and I_{corr} of the AZ91D magnesium alloy, the yttrium-based conversion coating and the silica sol-treated coating were presented in Table 2. The I_{corr} of the silica sol-treated coating is about $5.821E^{-7}A•cm^{-2}$, which decreased the corrosion current density about two orders of magnitude compared with the bare alloy and the yttrium-based conversion coating. Contrarily, the E_{corr} of the silica sol-treated sample is significantly shifted positively by about 230 mV compared to the AZ91D magnesium alloy, which means that the conversion coating after the silica sol treatment has better corrosion resistance. This is contributed to the remediation of the cracks by SiO_2, effectively prohibiting the magnesium alloy from contacting the etchant medium.

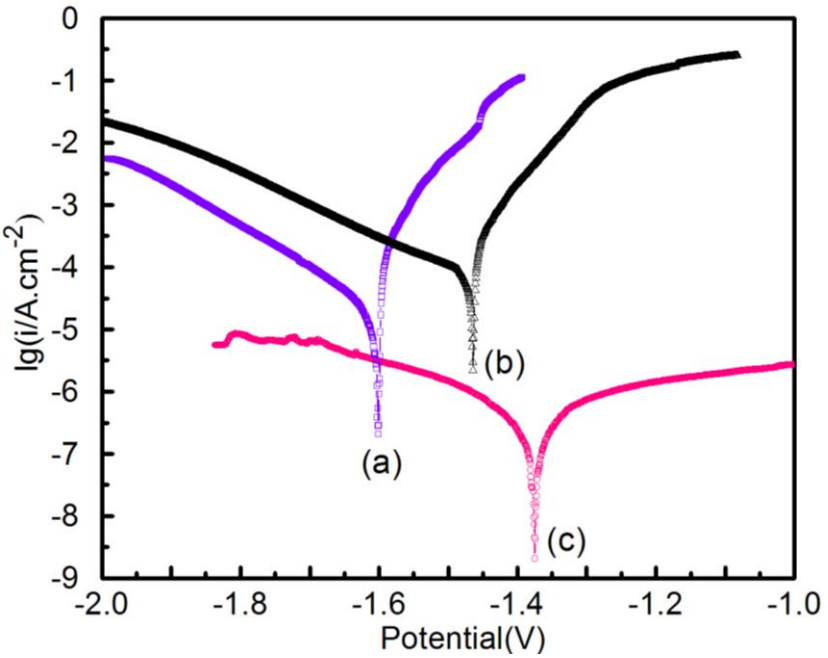

Figure 6. Potentiodynamic curves of (a) bare sample, (b) the coatings prepared in 10g/L $Y(NO_3)_3$ at 30 ℃ for 50min and (c) yttrium-based conversion coating dipped in 30% mass fraction of silica sol solution and naturally dried in air for 24 h followed by heating at 250 ℃ for 2 h

Table 2. Tafel fitting results of the potentiodynamic curves in Fig.6

Material	E_{corr}(mV)	I_{corr}/(A/cm^2)	bc(mV/dec)
The bare AZ91D magnesium alloy	-1600	7.025E-5	256.1
Conversion coating	-1460	5.880E-5	189.5
The yttrium-based coating post-treated with the silica sol	-1370	5.821E-7	164.8

To evaluate the corrosion resistance capability of the AZ91D magnesium alloy, the yttrium-based conversion coating and the sample covered by the conversion layer after treatment by the silica sol solution, electrochemical impedance spectroscopy (EIS) was conducted after the stabilization of the OCP immersion in 3.5 % NaCl solution at room temperature. As Nyquist plots shown in Fig.7, the bare alloy, the yttrium-based conversion coating and the sample with the silica-sol treated conversion coating show two capacitive loops at high and medium frequencies and an inductive loop at low frequencies, which means the same corrosion mechanism existed for both specimens. It can be seen that the obvious difference among the blank sample, the yttrium-based conversion coating and the post-treated sample is the size of the capacitive loop. The impendence of this capacitive loop of the post-treated sample exhibits an increase of 5× compared to AZ91D magnesium alloy substrate. The EIS plots in Fig.7 clearly reveal that the total impedance value of the sample with the silica-sol treated conversion coating is much higher than the bare alloy and the conversion coating, underlying the former one has a better corrosion resistance than the blank sample.

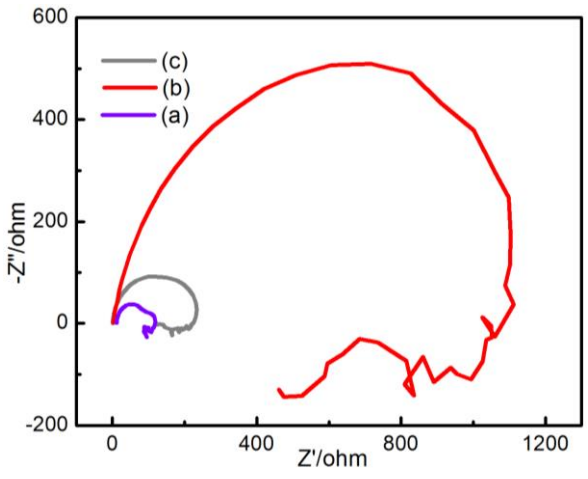

Figure 7. EIS spectra of (a) bare sample and (b) the coatings prepared in 10g/L $Y(NO_3)_3$ at 30 ℃ for 50min and (c) yttrium-based conversion coating dipped in 30% mass fraction of silica sol solution and naturally dried in air for 24 h followed by heating at 250 ℃ for 2 h

Fig.8 shows the morphology of the bare alloy and the sample with the silica-sol treated conversion coating after immersing in 3.5% NaCl solution for 72h at room temperature. General

corrosion and pitting corrosion were reflected in the immersion environment [39]. It was seen that the micro-structure of the conversion coating is porous, loose and uniform in Fig. 8a. The bare alloy could not provide an effective corrosion protection in the corrosive solutions. Whereas, on the surface of the sample with the silica-sol treated conversion coating, the irregular grids without deep holes appear in some area, while other areas are still intact, reflecting a superior capability of corrosion resistance. The results of the immersion tests further consolidate the results of the electrochemical tests.

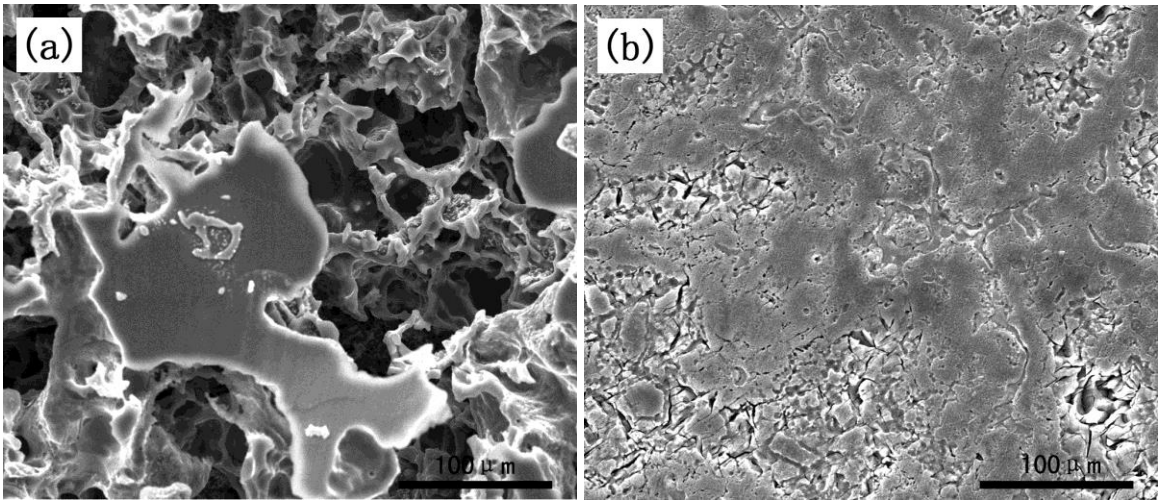

Figure 8. SEM surface morphology of the samples immersed in the 3.5%NaCl solution for 72h (a) bare sample and (b) the yttrium-based conversion coating dipped in 30% mass fraction of silica sol solution and naturally dried in air for 24 h followed by heating at 250 ℃for 2 h

4. CONCLUSIONS

A compact yttrium-based rare earth conversion coating on the AZ91D Mg alloy was prepared by simply immersing in a solution of yttrium nitrate firstly and then in a silica sol solution. The results are summarized as following:

(1) Under the optimal preparation process, the yttrium-based conversion coating is mainly composed of Y_2O_3, YOx/y, Al_2O_3 and MgO.

(2)The electrochemical tests and the immersion test show that the silica sol-treated yttrium-based conversion coating greatly improved the corrosion-resistance of the AZ91D Mg alloy. The corrosion potential shifted positively about 230 mV and the corrosion current density decreased about two orders of magnitude.

ACKNOWLEDGEMENT
This work was supported by the Ground Plan of Science and Technology Projects of Jiangxi Province, China (Grant No. KJLD2013078) and Open Project of Jiangxi Provincial Engineering Research Center for Magnesium Alloys, 2015.

References

1. B. P. Zhang, Y. F. Tu, J. Y. Chen, H. L. Zhang, Y. L. Kang and H. G. Suzuki, *J. Mater. Process. Technol.*, 184 (2007) 102.
2. E. M. Gutman, A. Eliezer, Y. Unigovski and E. Abramov, *Mater. Sci. Eng. A*, 2001, 302 (2001) 63.
3. W. W. Song, H. J. Martin, A. Hicks, D. Seely, C.A.Walton, W. Lawrimore, P.T. Wang and M.F. Horstemeyer, *Corros.Sci.*, 78 (2014) 353.
4. B. Ramezanzadeh, H. Vakili and R. Amini, *J. Ind. Eng. Chem.*, 30 (2015) 225.
5. A. H. Yi, J. Du , J. Wang, S. I. Mu, G. G. Zhang and W. F. Li, *Surf. Coat. Technol.*, 276 (2015) 239.
6. D. F. Zhang, Y. N. Gou, Y. P. Liu and X. X. Guo, *Surf. Coat. Technol.*, 236 (2013) 52.
7. L. Q. Zhu, Y. H. Li and W. P. Li, *Surf. Coat. Technol.*, 202 (2008) 5853.
8. D. L. Yan, G. Yu, B. N. Hu, J. Zhang, Z. W. Song and X. Y. Zhang, *J. Alloys Compd.*, 653 (2015) 271.
9. Y. Mao, Z. G. Li, K. Feng , X. W. Guo, Z. F. Zhou and Y. X. Wu, *J. Mater. Process. Tech.*, 219 (2015) 42.
10. L. K. Yu and H. C. Kuang, *Surf. Coat. Technol.*, 283 (2015) 194.
11. C. Christoglou, N. Voudouris, G. N. Angelopoulos, M. Pant and W. Dahl, *Surf. Coat. Technol.*, 184 (2004) 149.
12. S. Hiromoto, *Corros. Sci.*, 100 (2015) 284.
13. J. L. Davies, C. F. Glover, J. Van de Langkruis, E. Zoestbergen and G. Williams, *Corros. Sci.*, 100 (2015) 607.
14. M. F. Montemor, A. M. Simoes and M. J. Carmezim, *Appl. Surf. Sci.*, 253 (2007) 6922.
15. L. H. Yang, J. Q. Li, X. Yu, M. L. Zhang and X. M. Huang, *Appl. Surf. Sci.*, 255 (2008) 2338.
16. M. Dabala, K. Brunelli, E. Napolitani and M. Magrini, *Surf. Coat. Technol.*, 172 (2003) 227.
17. S. Pommiers, J. Frayret , A. Castetbon and M. Potin-Gautier, *Corros. Sci.*, 2014, 84 (2014) 135.
18. Z. L. Zou, N. Li , D. Y. Li, H. P. Liu and S. L. Mu, *J. Alloys Compd.*, 509 (2011) 503.
19. B. Valdez, S. Kiyota, M. Stoytcheva, R. Zlatev and J. M. Bastidas, *Corros. Sci.*, 87 (2014) 141.
20. H. D. Johansen, C.M.A. Brett and A.J. Motheo, *Corros. Sci.*, 63 (2012) 342.
21. B. Ramezanzadeh, H. Vakili and R. Amini, *J. Ind. Eng. Chem.*, 30 (2015) 225.
22. X. M. Wang, L. Q. Zhu, X. He and F. L. Sun, *Appl. Surf. Sci.*, 280 (2013) 467.
23. Y. J. Shun, R. C. Yu and S. L. Chao, *Corros. Sci.*, 93 (2015) 301.
24. Y. I. Choi, S. Salman, K. Kuroda and M. Okido, *Electrochim. Acta.*, 97 (2013) 313.
25. N. V. Murillo-Gutiérrez , F. Ansart, J-P. Bonino, M-J. Menu and M. Gressier, *Surf. Coat. Technol.*, 232 (2013) 606.
26. J. Y. Hu, Q. Li , X. K. Zhong, L. Zhang, B. Chen, *Prog. Org. Coat.*, 66 (2009) 199.
27. K. A. Yasakau , S. Kallip, M. L. Zheludkevich and M. G. S. Ferreira, *Electrochim. Acta.*, 112 (2013) 236.
28. A. S. Hamdy, *Mater. Lett.*, 60 (2006) 2633.
29. G. Jin, Y.Y. Yang, X.F. Cui, E.B. Liu, Z.Y. Wang and Q.F. Li, *Mater. Lett.*, 65 (2011), 1145.
30. X.F. Cui, Y.Y. Yang, E.B. Liu, G. Jin, J.G. Zhong and Q.F. Li, *Appl. Surf. Sci.*, 257(2011)9703.
31. J. R. Liu, Y. N. Guo and W. D. Huang, *Surf. Coat. Technol.*, 201 (2006) 1536.
32. J. Hayoz, T. Philo, M. Bovet, A. Züttel, S. Guthrie, G. Pastore, L. Schlapbach and P. Aebi, *J. Vac. Sci. Technol. A*, 18 (2000) 2417.
33. G. Gong and A. Atrens, *Adv. Eng. Mater.*, 5 (2003) 837.
34. A. Decroly and J. P. Petitjean, *Surf. Coat. Technol.*, 194 (2005) 1.
35. D. Seifzadeh and Z. Rajabalizadeh, *Surf. Coat. Technol.*, 218 (2013) 119.
36. R. Y. Zhang, S. Cai, G. H. Xu, H. Zhao, Y. Li, X. X. Wang, K. Huang, M. G. Ren and X. D. Wu, *Appl. Surf. Sci.*, 313 (2014) 896.

37. Z. Rajabalizadeh and D. Seifzadeh, *Progt. Met. Phys. Chem.*, 50 (2014) 516.
38. X. W. Yang, G. X. Wang, G. J. Dong, F. Gong and M. L. Zhang, *J. Alloys Compd.*, 487 (2009) 64.
39. H.J. Martin, M.F. Horstemeyer and P.T. Wang, *Corros. Sci.*, 53 (2011) 1348.